Physics Letters A ••• (••••) •••–•••

Contents lists available at ScienceDirect

Physics Letters A

www.elsevier.com/locate/pla

Nanoscale thermal cloaking by in-situ annealing silicon membrane

Yida Liu, Yanhua Cheng, Run Hu *, Xiaobing Luo

School of Energy and Power Engineering, Huazhong University of Science and Technology, Wuhan 430074, China

ARTICLE INFO

Article history:
Received 20 February 2019
Received in revised form 15 April 2019
Accepted 18 April 2019
Available online xxxx
Communicated by R. Wu

Keywords:
Molecular dynamics
Thermal cloak
In-situ annealing
Phonon localization

ABSTRACT

With the advent of thermal metamaterials, many new thermal functionalities have been proposed, like thermal cloaking, concentrating, etc. However, these thermal functionalities are based on the transformation thermotics or scattering cancellation technique, which, derived from Fourier's law, cannot apply to the micro-/nanoscale counterparts. In this paper, we design a nanoscale thermal cloak based on a crystalline silicon (Si) membrane and investigate the in-plane phonon transport via non-equilibrium molecular dynamics (NEMD) simulation by in-situ tuning the thermal conductivity of the thermal cloak from crystalline Si to amorphous Si. The two-dimensional temperature profile is obtained, and the thermal cloaking effect is evaluated by the ratio of heat flux. By analyzing the phonon density of state (PDOS) and the mode participation ratio (MPR), the mechanism can be attributed to the phonon localization in the annealed cloaking region. The proposed nanoscale thermal cloak by in-situ tuned thermal conductivity, may trigger the development of nanoscale thermal functionalities and open avenues for and thermal management for nano-photonics and nano-electronics.

1. Introduction

Along with research history of heat transfer, heat has long been considered to be transferred in the diffusive way, which is hard to control in the directional management [1–7]. Thanks to the advent of thermal metamaterials, such deep-rooted barrier has been relieved and many new thermal functionalities are successively proposed thereby, such as thermal cloaking [1–5], concentrating [8,9], camouflage [10–12], refraction [13], reflection [14], encoding [15], diode [16], etc. Among them, the most beautiful one is, beyond all doubt, thermal cloaking, which, derived from its optical invisibility cloak counterpart, can tune the heat flux to pass around central region without disturbing the outside temperature field, just like passing through a homogenous plane. In such way, the objects sitting inside the central region can be concealed from an exterior infrared camera. To design such thermal cloak, there are two frequently used methods, i.e. the transformation thermotics and the scattering cancellation methods. In the transformation thermotics, the virtual space is transformed into the real space with inhomogeneous material makeup for the cloak by the seminal formula $\kappa' = \mathbf{\Lambda}\kappa_0\mathbf{\Lambda}^{\mathrm{T}}/\det(\mathbf{\Lambda})$, where Λ is the Jacobian matrix and $\mathbf{\Lambda}^{\mathrm{T}}$ is the transpose of $\mathbf{\Lambda}$, κ_0 is the original thermal conductivity [17]. In the scattering cancellation method, the thermal conductivity of the cloak is designed based on $\kappa_2 = \frac{\kappa_b(2R_2^3+R_1^3)}{2(R_2^3-R_1^3)}$, where R_1 and R_2 are the inner and outer radii of the cloak, κ_2 and κ_b are the thermal conductivity of the cloak and the background [3,4]. Since these formulas are derived from the Fourier's law, these two methods only deal with the macroscale cloaks, and many other functionalities, achieved by these two methods, are also in the macroscale regime. Moreover, to fabricate the inhomogeneous metamaterials, the effective medium approximation (EMA) is frequently used with neglecting the interfacial thermal resistance, but the obtained effective thermal conductivity tensors are usually less anisotropic as those predicted by the transformation thermotics [8,10]. As a result, the experimental thermal functionalities are usually not as perfect as those in theory.

In contrast, the microscale thermal functionalities are much limited. Due to the wave-particle duality of phonons, as the heat carrier in the microscale, some new functionalities are proposed in a different realm, such as quantum thermal rectification, quantum heat shuttling, topological phonon Hall effect, etc. [18–24]. The macroscale thermal functionalities are hard to find the counterparts in the microscale, but this does not mean impossible. Ye et al. reported the thermal properties of thermal cloaking in graphene via chemical functionalization in nanoscale [25]. Though effective, the chemical functionalization technique is complicated for practical processing. Recently, Zhao et al. engineered the thermal conductivity of Si nanowire by transforming the morphology of crystal Si to amorphous Si using helium ion irradiation, from

* Corresponding author.
E-mail address: hurun@hust.edu.cn (R. Hu).

https://doi.org/10.1016/j.physleta.2019.04.038
0375-9601/

the intrinsic value (~50 $Wm^{-1}K^{-1}$) to the amorphous value (~1.7 $Wm^{-1}K^{-1}$), which enables it a practical way to change the in-situ thermal conductivity of Si on the micro/nanoscale [26]. Such in-situ tuning of thermal conductivity could overcome the drawback of EMA, and achieve more perfect thermal functionality than the macroscale ones.

Inspired by the advantages of the in-situ tuning of local thermal conductivity, we would like to explore the thermal cloaking functionality in a nanoscale Si membrane. We designed a nanoscale thermal cloak on a Si membrane, and the annular cloak is composed of amorphous Si which is transformed by crystalline Si after in-situ annealing. Non-equilibrium molecular dynamics (NEMD) simulations are used to analyse the performance of thermal cloaking and in-plane phonon transport. The widths of the annealed cloaks are discussed with revealing the underlying mechanism. The proposed nanoscale thermal cloak by in-situ tuned thermal conductivity, may trigger the exploration of the thermal functionality counterparts in the nanoscale, and be used for thermal management for nano-photonics and nano-electronics.

2. Molecular dynamics

Our NEMD simulations are conducted by using the LAMMPS packages. The interatomic interactions of Si atoms in membrane are modelled by the Tersoff potential [27]

$$E = \frac{1}{2}\sum_i \sum_{j\neq i} f_C\left(r_{ij}\right)\left[f_R\left(r_{ij}\right) + b_{ij} f_A\left(r_{ij}\right)\right], \tag{1}$$

where E represents the total energy of the system, r_{ij} represents the distance between atom i and atom j. The function f_R denotes a repellent pair potential, f_A denotes an attractive pair potential, f_C is just a smooth cutoff function aimed to limit the range of the potential. As for the function b_{ij}, it is used to measure the bond order. The structure schematic of the Si membrane with a thermal cloak model is shown in Fig. 1. Similar to the popular design at the macroscale, the shape of the thermal cloak was designed as a ring with uniform thickness. In our simulation, the lattice constant of Si is set to 5.54 Å, and the initial membrane is constructed from crystalline Si with 2×60×40 unit cells (UC) in the x, y, and z directions, respectively. After annealing, the cloak region consists of amorphous Si, while the rest is still composed of crystalline Si. We have divided our system into three regions: the fixed region, the thermostat region and the central region. The thickness of the fixed region at both ends of the membrane along the y-axis is as 2 UC, where the atoms are fixed in order to prevent the bulk motion of the whole system. Adjacent to the fixed region is the thermostat region which is set to 8 UC long along y-axis; in this region atoms are maintained at high and low temperature respectively at both sides by Nose–Hoover thermostats as follows [28]

$$\frac{d}{dt}p_i = F_i - \gamma p_i, \tag{2.1}$$

$$\frac{d}{dt}\gamma = \frac{1}{\tau^2}\left[\frac{T(t)}{T_0} - 1\right], \tag{2.2}$$

$$T(t) = \frac{2}{3Nk_B}\sum_i \frac{p_i^2}{2m_i}, \tag{2.3}$$

where p_i, m_i, F_i, denote the momentum, mass and force of atom i respectively, γ represents the dynamic parameters, τ represents the relaxation time, k_B is the boltzmann constant and N denotes the total number of atoms in the thermostat.

The simulation process can be divided into two steps: the first is the annealing process and the second is the NEMD process. The

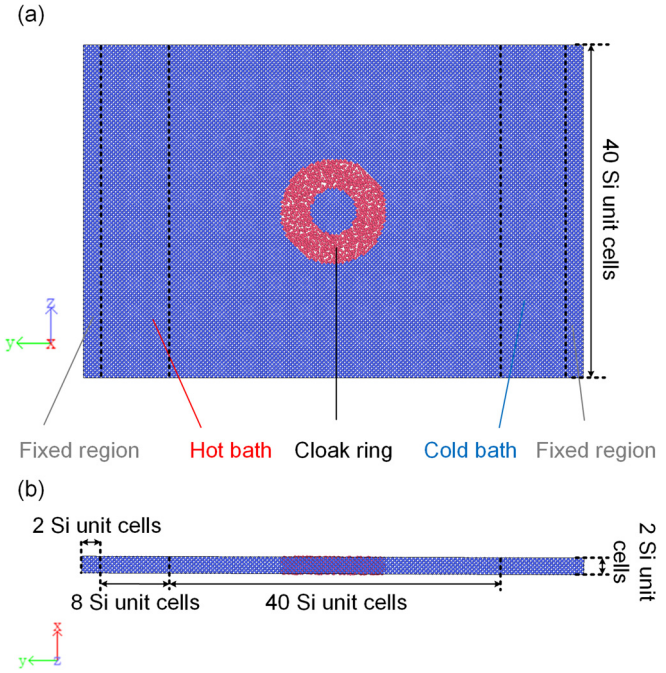

Fig. 1. (a) Top view and (b) side view of the membrane and its regional distribution. Due to the atom mixing during the annealing process, the atoms in the cloak region are chaotic. In contrast, the crystalline Si atoms are orderly distributed outside the cloak region. Colours are only used to guide eye for the nanoscale thermal cloak.

annealing procedure is similar to that outlined in Refs. [29,30]. The time step is set at 1 fs. In the first step, we fixed the atoms that are outside the cloak ring region in the central region, so as to prevent the heat from affecting the atoms in other region. Then the initial crystalline Si atoms in the cloak ring region are heated to 4000 K and equilibrate for 50 ps, which convert them from a solid state to a liquid state, afterwards we quench the atoms in this region at a rate of 6.7×10^{15} K/s. When the temperature reaches about 100 K the quenching procedure is stopped. Then we iteratively adjusted the atomic coordinates to minimize the energy of the system based on the backtracking method which is described in Nocedal and Wright's Numerical Optimization [31]. The minimization is stopped when all the components of force on atoms are less than 10^{-3} eV/Å. Fig. 2(b) shows the length of force vector for all atoms variation during minimization. In this way, the atoms in the cloak ring region have been transformed from crystalline state to amorphous state. Fig. 2(a) shows the temperature variation in cloak ring region during annealing. In the second step, firstly, we unfix the atoms in the central region and give all atoms a random velocity vector. Then the system is relaxed in the NPT ensemble at zero pressure with temperature increasing from 100 K to 300 K for 50 ps, afterwards the system is equilibrated in the NPT ensemble at zero pressure and 300 K temperature for 100 ps. Finally, the NEMD method is performed in this system for 800 ps, and the temperature of the hot bath and cold bath is 350 K and 250 K respectively. During the NEMD procedure, the temperature and heat flux of the atoms in the thermal region are recorded for subsequent analysis. The temperature of each atom is calculated by

$$\sum_i \varepsilon_i = \frac{dim}{2}k_B N T, \tag{3}$$

in which, ε_i represents the kinetic energy of atom i, dim is dimensionality of the simulation and in our system $dim = 3$, k_B is the boltzmann constant, N denotes the atomic number. Then the heat flux is calculated by

Please cite this article in press as: Y. Liu et al., Nanoscale thermal cloaking by in-situ annealing silicon membrane, Phys. Lett. A (2019), https://doi.org/10.1016/j.physleta.2019.04.038

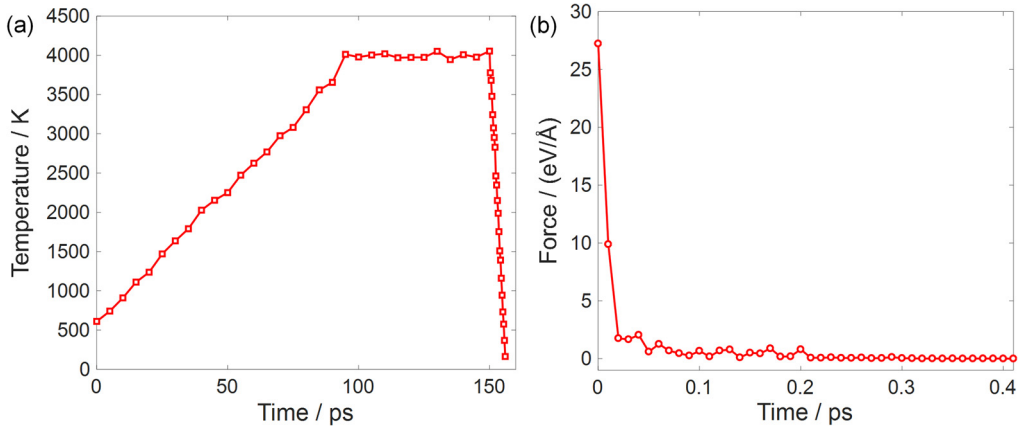

Fig. 2. (a) Temperature variation in cloaking region during the annealing process, and (b) energy minimization process.

$$\mathbf{J} = \frac{1}{V}\left[\sum_i e_i \mathbf{v}_i - \sum_i \mathbf{S}_i \mathbf{v}_i\right], \tag{4}$$

where **J** denotes the heat flux, e_i in the first term of the equation is the energy per atom including the potential and kinetic energy, $\mathbf{S}_i$ in the second term of the equation is the stress tensor per atom which has 9 components: *xx*, *xy*, *xz*, *yy*, *yx*, *yz*, *zz*, *zx* and *zy*. $\mathbf{v}_i$ is the velocity vector per atom and V represents the volume of this region. The heat flux in three directions can be expressed as follows

$$J_x = \frac{1}{V}\left[\sum_i e_i v_{xi} - \sum_i \left(S_{ixx} v_{ix} + S_{ixy} v_{iy} + S_{ixz} v_{iz}\right)\right], \tag{5.1}$$

$$J_y = \frac{1}{V}\left[\sum_i e_i v_{yi} - \sum_i \left(S_{iyx} v_{ix} + S_{iyy} v_{iy} + S_{iyz} v_{iz}\right)\right], \tag{5.2}$$

$$J_z = \frac{1}{V}\left[\sum_i e_i v_{zi} - \sum_i \left(S_{izx} v_{ix} + S_{izy} v_{iy} + S_{izz} v_{iz}\right)\right]. \tag{5.3}$$

3. Results and discussions

To identify the working performance of the nanoscale thermal cloak, we built three different models for comparison, as shown in Fig. 3(a-c), including Si membrane without, with 1-nm-thickness, and with 2-nm-thickness thermal cloak rings. Except for the thickness difference, other conditions in our simulations are all the same. The outer diameters of the thermal cloaks are maintained the same as 7 nm. Fig. 3(d-f) show the two-dimensional temperature field of the three models. To ensure the validity of the temperature field, the temperature of each atom is an average of 400 ps. The dotted black line denotes the approximate position of the cloak ring on the membrane. It is apparent that the temperature of atoms in the central region is relatively uniform, which reveals the existence of the thermal cloaking effect. Through the comparison between Fig. 3(e) and Fig. 3(f), we notice that the central region in the membrane with 2 nm cloak ring has a more pronounced outline, which may indicate better cloaking performance with wider thermal cloak ring.

Fig. 3(g-i) show the *y*-*z* plane heat flux field of the three models. Since the temperature difference along the *x* and *z* directions of the system is subtle, the heat flux is negligible. Therefore, we only show the magnitude of the heat flux in the y direction by using Eq. (5.2). The heat flux of each atom is an average of 400 ps. For the 1 mm ring membrane, the heat flux field is inhomogeneous. To compare the difference, we divided the heat flux into the upper, middle and lower parts. Due to the symmetry, we are only concerned with the top and the middle parts. The heat flux in the middle part is much less than that in the upper part, indicating that more heat flux passes around the cloak ring region. For the 2 nm ring membrane, we notice that besides that the heat flux distribution is roughly the same, the heat flow in the middle part of the 2 mm ring membrane is less than that in the middle part of the 1 mm ring membrane. And this phenomenon is a good confirmation that the 2 nm cloak ring has a better thermal cloaking performance than the 1 nm cloak ring. As shown in Fig. 4(a), we use white lines to frame two rectangular regions A and B in the upper part and the middle part, and the region B is in the cloaking region. In order to quantify the thermal cloaking performance, we calculate the ratio of thermal cloaking (RTC)

$$\mathrm{RTC} = \frac{J_A}{J_B} \tag{6}$$

where J_A and J_B is the average heat flux through region A and region B, respectively. For a perfect membrane, RTC = 1. For a perfect thermal cloak, there is no heat flux in the region B, thus $J_B = 0$ and RTC should be infinity. By this definition, RTC becomes an index positively correlated with the thermal cloaking performance. The higher RTC is, the better the thermal cloaking performance will be. Fig. 4(b) shows the RTC of membrane with different cloak ring width. As the cloak ring width increases, the RTC increases monotonously, which accords with our analysis above. To sum up, we can draw a preliminary conclusion that the thermal cloaking performance is positively proportional to the width of the cloak ring.

To explore the mechanism of nanoscale thermal cloak, we calculate the phonon density of states (PDOS) in an annular region outside the cloaking region. In addition, in order to control for the same regional variable, the annular region we used to calculate PDOS in three samples are exactly the same. Thus we use the cloak ring region in 2 nm ring membrane as a standard computational domain. The PDOS is derived from the Fourier transform of the velocity autocorrelation function as

$$\mathrm{PDOS}(\omega) = \frac{1}{N\sqrt{2\pi}} \int e^{-i\omega t} \left\langle \sum_{j=1}^{N} \mathbf{v}_j(0)\, \mathbf{v}_j(t) \right\rangle \mathrm{d}t \tag{7}$$

where $\mathbf{v}_j$ is velocity vector of atom j, N is total atom number in the system, ω represents phonon frequency. Fig. 3(j) shows the PDOS of specific atoms in the perfect membrane. There is a strong peak at high frequency 15 THz and a weak peak at low frequency 4.5 THz respectively, which agrees with previous studies and corresponds to the crystalline Si [32]. As for the 1 nm ring membrane

Please cite this article in press as: Y. Liu et al., Nanoscale thermal cloaking by in-situ annealing silicon membrane, Phys. Lett. A (2019), https://doi.org/10.1016/j.physleta.2019.04.038

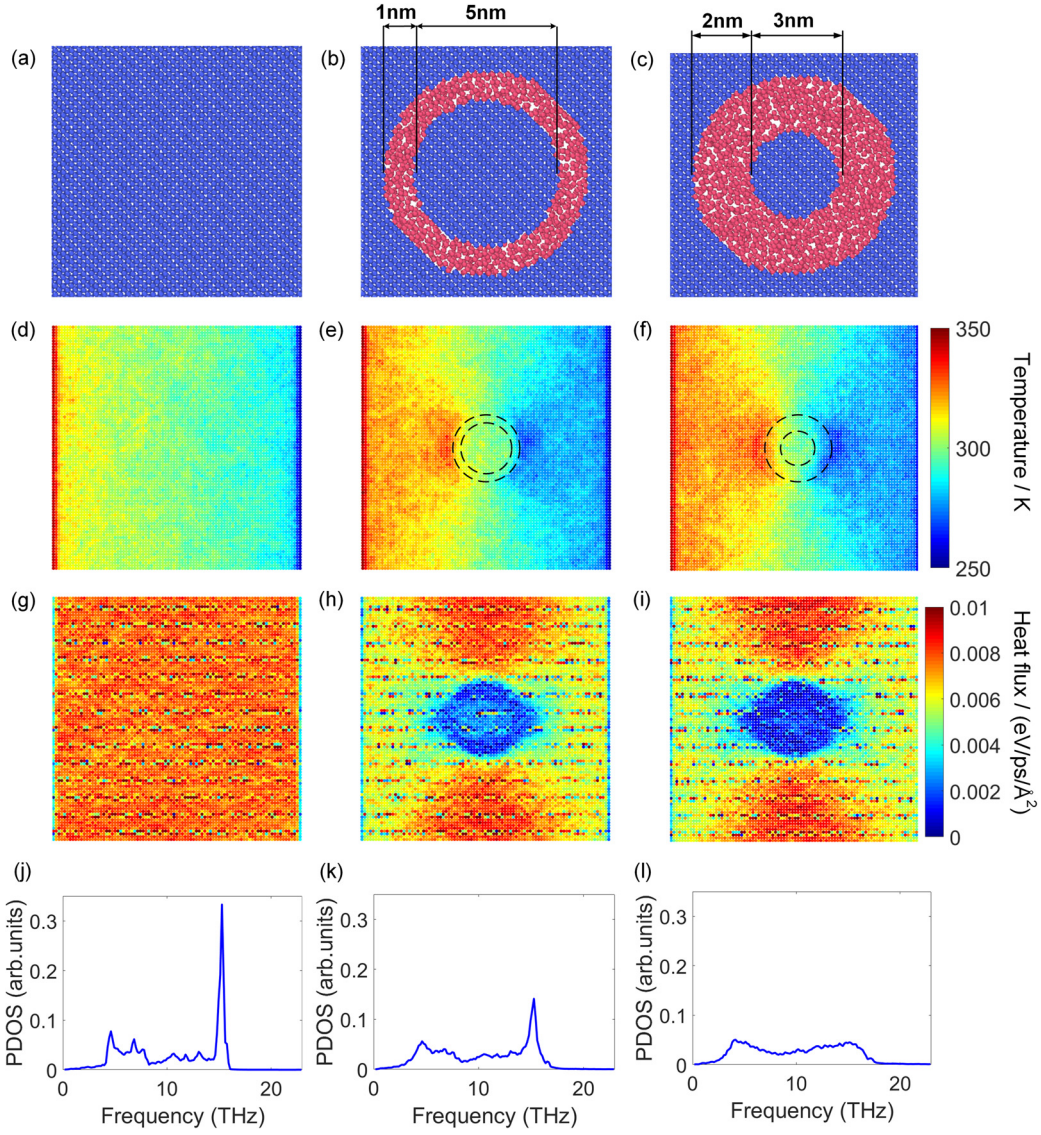

Fig. 3. Detailed atomic model diagram of (a) perfect membrane, (b) 1 nm cloak ring membrane, (c) 2 nm cloak ring membrane. Two-dimensional temperature field of (d) perfect membrane, (e) 1 nm cloak ring membrane, (f) 2 nm cloak ring membrane. The black dotted line is the approximate position of the cloak ring. Two-dimensional heat flux field of (g) perfect membrane, (h) 1 nm cloak ring membrane, (i) 2 nm cloak ring membrane. PDOS in annular region of (j) perfect membrane, (k) 1 nm cloak ring membrane, (l) 2 nm cloak ring membrane.

and 2 nm membrane shown in the Fig. 4(k-l), the peak of the high frequency region is weakened, corresponding to the increase of the amount of modes in the low frequency region. This results from that the amorphous Si atoms have lower vibration frequencies. By comparing Fig. 3(j) with Fig. 3(l), we find that the crystalline Si atoms show a strong peak corresponding to optical phonons at 15 THz, while the amorphous ones show a large amount of modes ranging from 3 THz to 7 THz. In order to explain for the difference in PDOS, we calculate the mode participation ratio (MPR) as [33]

$$\mathrm{MPR}(\omega) = \frac{1}{N}\frac{\left[\sum_i \mathrm{PDOS}_i(\omega)^2\right]^2}{\sum_i \mathrm{PDOS}_i(\omega)^4} \tag{8}$$

where the $\mathrm{PDOS}_i(\omega)$ is the local density of states of ith atom based on Eq. (7), and N represents total number of atoms in the system. In Fig. 4(c), we compare the MPR of crystalline Si membrane (blue dots), Si membrane with 1-nm-thickness (red dots) and 2-nm-thickness (yellow dots) thermal cloak rings. Compared with crystalline Si membrane, there is a clear reduction of MPR in membrane with cloak ring for both low and high frequency phonons. For crystalline Si membrane, most MPR values are above 0.5, implying that these phonon modes are delocalized. As for membrane with cloak ring, most values are below 0.5, implying the localized phonon modes [34]. The results confirm that phonon localizations account for the thermal conductivity reduction in amorphous Si. The low thermal conductivity of amorphous Si has a great impact on the heat flux field distribution of the membrane, which makes the heat flux passes around the thermal cloak ring region, and the cloaking region is shielded from the heat flux. By comparing MPR of Si membrane with 1 nm cloak ring and that with 2 nm cloak ring, the MPR value of the latter is generally slightly smaller, implying the weaker phonon localization. The reason is that only half of the Si atoms in annular region of 1 nm ring membrane are composed with amorphous Si and others are crystalline Si, while the atoms in annular region of 2 nm ring membrane are all composed with amorphous Si. Through such analyses, we find that the thermal cloaking effect is correlated with the phonon localization in the specific annular region, and stronger localization indicates better thermal cloaking performance.

Please cite this article in press as: Y. Liu et al., Nanoscale thermal cloaking by in-situ annealing silicon membrane, Phys. Lett. A (2019), https://doi.org/10.1016/j.physleta.2019.04.038

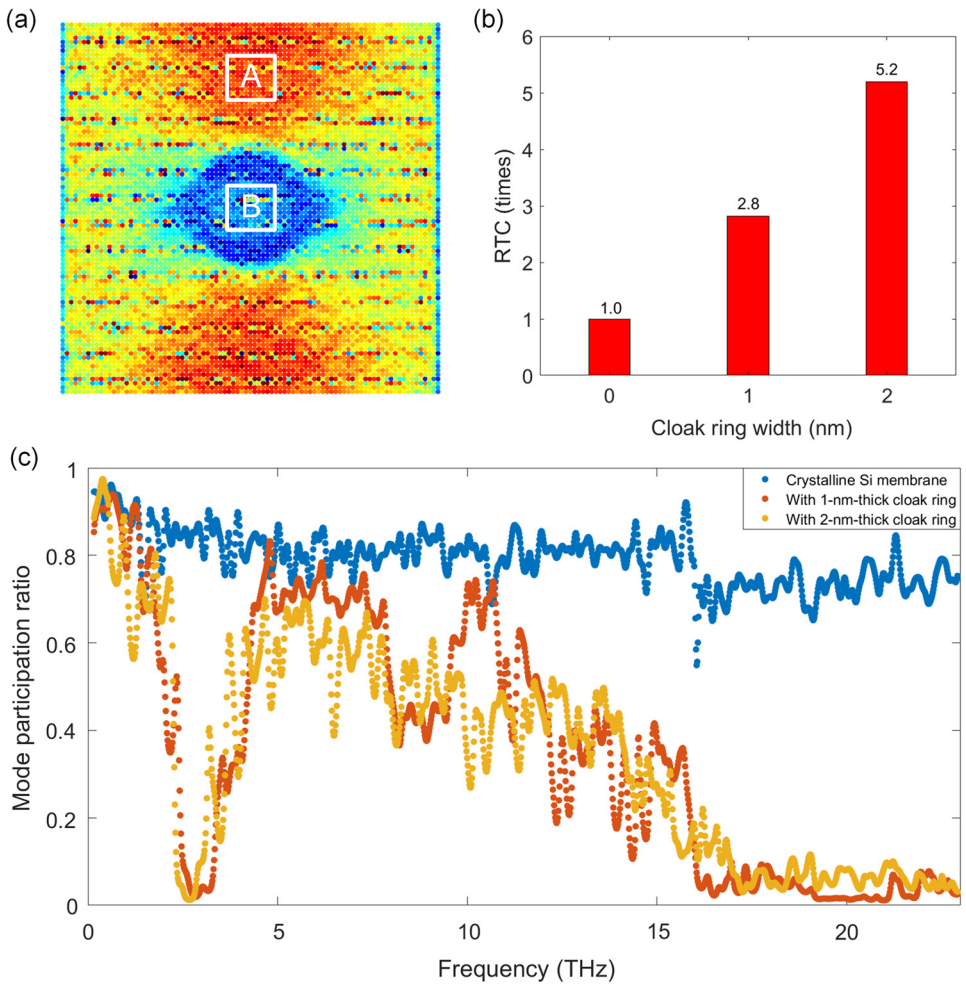

Fig. 4. (a) Partition diagram in a heat flux field, (b) RTCs of membrane with different cloak ring width, (c) mode participation ratio in annular region with different cloak ring width. (For interpretation of the colours in the figure(s), the reader is referred to the web version of this article.)

4. Conclusions

In summary, to explore the counterpart of the macroscale thermal functionalities in the nanoscale, we propose a nanoscale thermal cloak on a silicon (Si) membrane and analyse its underlying mechanism. The cloak region is formed by amorphous Si and 'melt-and-quench' technique is used to in-situ turn crystalline Si to amorphous state. Non-equilibrium molecule dynamics (NEMD) simulations were carried out to compare the temperature fields of perfect membrane, 1 nm and 2 nm thermal cloaking ring membrane to identify the thermal cloaking effect. The consequence of a nanoscale thermal cloaking effect is similar is to the macroscale one that the heat flux will pass around the cloaking region. Our results indicate that the thermal cloaking effect is positively proportional to the width of the cloak ring. The underlying mechanism of nanoscale thermal cloaking is explored by calculating PDOS and MPR. We find that the phonon localization occurs in the thermal cloak ring region and accounts for the reduction of thermal conductivity of the amorphous Si. The proposed method to design nanoscale thermal cloak by in-situ tuning the atomic lattice structure of the material is more practical and effective, and may open avenues for nanoscale thermal functionalities and thermal management for nano-photonics and nano-electronics.

Acknowledgements

The authors would like to acknowledge the financial support by National Natural Science Foundation of China (51606074, 51625601), and the Ministry of Science and Technology of the People's Republic of China (Project No. 2017YFE0100600).

References

[1] C.Z. Fan, Y. Gao, J.P. Huang, Appl. Phys. Lett. 92 (2008) 251907.
[2] D.M. Nguyen, H. Xu, Y. Zhang, B.L. Zhang, Appl. Phys. Lett. 107 (2015) 121901.
[3] T. Han, X. Bai, D. Gao, J.T.L. Thong, B.W. Li, C.W. Qiu, Phys. Rev. Lett. 112 (2014) 054302.
[4] H. Xu, X. Shi, F. Gao, H. Sun, B. Zhang, Phys. Rev. Lett. 112 (2014) 1.
[5] L.L. Zhou, S.Y. Huang, M. Wang, R. Hu, X.B. Luo, Phys. Lett. A 383 (2019) 759–763.
[6] Y.P. Ma, W. Lan, B. Xie, R. Hu, X.B. Luo, Int. J. Heat Mass Transf. 116 (2018) 694–702.
[7] B.F. Shang, Y.P. Ma, R. Hu, C. Yuan, J.Y. Hu, X.B. Luo, Appl. Therm. Eng. 118 (2017) 593–599.
[8] R. Hu, X.L. Wei, J.Y. Hu, X.B. Luo, Sci. Rep. 4 (2014) 3600.
[9] F. Chen, D.Y. Lei, Sci. Rep. 5 (2015) 11552.
[10] R. Hu, S.L. Zhou, Y. Li, D.Y. Lei, X.B. Luo, C.W. Qiu, Adv. Mater. 30 (2018) 1707237.
[11] T.C. Han, X. Bai, J.T.L. Thong, B.W. Li, C.W. Qiu, Adv. Mater. 26 (2014) 1731–1734.
[12] S.L. Zhou, R. Hu, X.B. Luo, Int. J. Heat Mass Transf. 127 (2018) 114–121.
[13] R. Hu, B. Xie, J.Y. Hu, Q. Chen, X.B. Luo, Europhys. Lett. 111 (2015) 54003.
[14] R. Hu, S. Zhou, W. Shu, B. Xie, Y. Ma, X.B. Luo, AIP Adv. 6 (2016) 125111.
[15] R. Hu, S. Huang, M. Wang, L. Zhou, X. Peng, X.B. Luo, Phys. Rev. Appl. 10 (2018) 054032.
[16] Y. Li, X.Y. Shen, Z.H. Wu, J.Y. Huang, Y.X. Chen, Y.S. Ni, J.P. Huang, Phys. Rev. Lett. 115 (2015) 195503.
[17] S. Guenneau, C. Amra, D. Veynante, Opt. Express 20 (7) (2012) 8207.
[18] N. Li, J. Ren, L. Wang, G. Zhang, P. Hanggi, B.W. Li, Rev. Mod. Phys. 84 (2012) 1045–1066.
[19] M. Maldovan, Phys. Rev. Lett. 110 (2013) 025902.

Please cite this article in press as: Y. Liu et al., Nanoscale thermal cloaking by in-situ annealing silicon membrane, Phys. Lett. A (2019), https://doi.org/10.1016/j.physleta.2019.04.038

[20] Y. Wang, A. Vallabhaneni, J. Hu, B. Qiu, Y.P. Chen, X.L. Ruan, Nano Lett. 14 (2014) 592–596.
[21] S. Wang, A.L. Cottrill, Y. Kunai, A.R. Toland, P. Liu, W.J. Wang, M.S. Strano, Phys. Chem. Chem. Phys. 19 (2017) 13172.
[22] L.F. Zhang, J. Ren, J.S. Wang, Phys. Rev. Lett. 105 (2010) 225901.
[23] T. Qin, J.H. Zhou, J.R. Shi, Phys. Rev. B 86 (2012) 104305.
[24] Y.Z. Liu, Y. Xu, C. Shou, Phys. Rev. B 96 (2017) 064106.
[25] Z.Q. Ye, B.Y. Cao, Phys. Chem. Chem. Phys. 18 (2016) 32952.
[26] Y.S. Zhao, D. Liu, J. Chen, L.Y. Zhu, A. Belianinov, O.S. Ovchinnikova, R.R. Unocic, M.J. Burch, S. Kim, H.F. Hao, D.S. Pickard, B.W. Li, J.T.L. Thong, Nat. Commun. 8 (2017) 15919.
[27] J. Tersoff, Phys. Rev. B 39 (1989) 5566.
[28] H.J.C. Berendsen, J.P.M. Postma, W.F.V. Gunsteren, A. Dinola, J.R. Haak, J. Chem. Phys. 81 (1984) 3684.
[29] C. Fusco, T. Albaret, A. Tanguy, Phys. Rev. E 82 (2010) 066116.
[30] A. France-Lanord, E. Blandre, T. Albaret, S. Merabia, D. Lacroix, K. Termentzidis, J. Phys. Condens. Matter 26 (2014) 055011.
[31] J. Nocedal, S.J. Wright, Numerical Optimization, Springer, New York, 2006, see in particular procedure 3.1 on p. 41.
[32] H.P. Li, R.Q. Zhang, Europhys. Lett. 105 (2014) 56003.
[33] G.C. Loh, E.H.T. Teo, B.K. Tay, Diam. Relat. Mater. 23 (2012) 88–92.
[34] D.K. Ma, H.R. Ding, H. Meng, L. Feng, Y. Wu, J. Shiomi, N. Yang, Phys. Rev. B 94 (2016) 165434.

Please cite this article in press as: Y. Liu et al., Nanoscale thermal cloaking by in-situ annealing silicon membrane, Phys. Lett. A (2019), https://doi.org/10.1016/j.physleta.2019.04.038